CSIRO PUBLISHING

International Journal of Wildland Fire **2009**, *18*, 290–301 www.publish.csiro.au/journals/ijwf

A simple model for wind effects of burning structures and topography on wildland–urban interface surface-fire propagation

Ronald G. Rehm[A,C] *and William (Ruddy) Mell*[B]

[A]RGR Consulting, Limited Liability Corporation and National Institute of Standards and Technology, Building 224, Room B260, 100 Bureau Drive, Gaithersburg, MD 20899, USA.

[B]National Institute of Standards and Technology, Building 224, Room B246, 100 Bureau Drive, Gaithersburg, MD 20899, USA.

[C]Corresponding author. Email: ronald.rehm@nist.gov

Abstract. The present paper presents a simple model to demonstrate the effect on grass-fire propagation of the winds induced by structural fires in a wildland–urban interface setting. The model combines an empirical formula for wind-driven grass-fire spread and a physics-based analytical solution to the Euler equations to determine the ground-level wind produced by the burning structure. The scaling of the wind is based on the heat release rate of the structural fire as well as other parameters. Also considered are an ambient wind and a topographical wind, assumed to be proportional to the ground slope. Data on grass and structure fires required by the model are discussed. Fire front propagation predicted by this model is illustrated by three examples: a front passing a single burning structure on flat terrain, a front passing a burning structure on a hill, and a front passing several burning structures. The model predicts that a fire front will be accelerated toward the burning structure upon approach and decelerated after passing the structure. Several burning structures multiply the effects of an individual burning structure.

Introduction

Over the past few years, wildland–urban interface (WUI) fires have become of much greater concern. The WUI includes people and property, and therefore the costs of damage in the built environment, especially when measured in terms of injury to people, death and property damage, are far higher than in wildland settings (National Interagency Fire Center 2006*a*). The WUI has been found to be large and growing rapidly in the United States as population expands and housing development in wildland areas continues. People are building more houses in a wildland setting every year (Environmental Literacy Council 2007). For example, data from the year 2000 show that ~36% or 42 million homes in the USA are in the WUI and the numbers are growing rapidly (Gustafson *et al*. 2005; Radeloff *et al*. 2005). Also, as the average temperature both within the United States and globally has increased, earlier snowmelts have taken place, extending the number of weeks every year that forests are exposed to high temperatures and dangerously dry conditions (Andrews *et al*. 2007). Increasingly hot and dry conditions in the United States have led, in turn, to larger areas of wildland fuel consumed by wildfire with greater threat to the WUI (National Interagency Fire Center 2006*b*; Andrews *et al*. 2007).

The philosophy of management of wildlands in the United States has undergone a major change over the past few decades (Andrews *et al*. 2007; Berry 2007). Early in the twentieth century, management practice was to suppress wildfire completely. The 'Smokey the Bear' campaign emphasized reporting and suppression of all fire in wildland settings. This practice, in turn, allowed the buildup of near-ground vegetative material in forests, so that when a fire did occur, it burned with a much higher intensity than if this material had been expunged by more frequent, but less intense fires. Today, the philosophy is that fire is a naturally occurring process in forests and that periodic, low-intensity fires help to keep the forest floor clear of vegetative debris that can turn low-intensity fires into high-intensity ones. The forests that have been cleared periodically by small fires are now believed to be healthier and much more able to resist the negative effects of wildfire.

Observations show that WUI fires can behave differently than wildland fires (Murphy *et al*. 2007). Wildfires are found to spread as a fireline or fire front with distinct features, such as intensity, rate of spread (ROS), flame height. that depend on properties of the wildland fuel, the meteorological properties and topography. WUI fires are produced when wildfires invade a community. For example, Fig. 1 shows a photograph, taken by John Gibbins of the San Diego Post Tribune, of a wildland fire front approaching the Scripps Ranch residential community during the Cedar Fire in October 2003.

In both wildland and WUI fires, spot fires ignited by brands are a primary fire-spread mechanism. In WUI fires, brands can ignite a house, producing a vigorous structure fire and substantial additional brand production while the surrounding trees remain untouched. Examples of such behavior, including photographs, are presented in the USDA report on the Angora Fire that occurred south-west of Lake Tahoe during 24–26 June 2007 (Murphy *et al*. 2007). The brands were estimated to travel up to

 10.1071/WF08087 1049-8001/09/030290

Fig. 1. Photograph of a fire front approaching the Scripps Ranch residential community during the Cedar Fire in October 2003. (Photograph by John Gibbins of the San Diego Post Tribune.)

~0.4 km (1/4 mile) downwind in this fire and were suspected of igniting additional houses.

Although the danger and costs of WUI fires have increased dramatically (National Interagency Fire Center 2006*a*), the tools to address these fires have not been developed (Mell *et al*. 2007). The length and time-scales associated with wildland and WUI fires vary greatly, ranging from the millimetre length scales and subsecond time-scales associated with combustion of fuel elements to tens of kilometres and days associated with smoke transport and total burned area. This wide variation in scales, coupled with the highly non-linear behavior of many of the physical processes represents the major challenge faced in attempting to model such fires.

Models that hope to predict WUI rather than wildland fire spread are likely to be more complex because of the heterogeneity of the fuel. The usual conceptual models for the interaction of a wildfire with structures regard the structures as isolated and surrounded by wildland fuels and imply a density of houses that is so low that the burning of these houses has no effect on the progression of the wildfire (GAO 2005).

In reality, often there are many burning structures in addition to the wildfire itself that can contribute to the fire spread. For example, in the photograph of Gibbins (Fig. 1), imagine that some unburned structures were to be ignited by brands (or other means). Also assume that the fire front were to invade the community. (The Cedar Fire actually did not invade the community because a road acted as a fire break.) Such a scenario is an example of the type of WUI fire envisioned for the analysis presented here.

Currently operational models might be satisfactory for some predictions of large wildfire behavior, where average data on wildland fuels is available from Geographical Information Systems (GIS) over elements measuring 30 m per side. Likewise, predictions of wildland or WUI fire behavior over areas measuring a few kilometres per side using field models might soon be possible, provided the detailed data necessary to make such predictions can be obtained. However, it is very unlikely that the capability for useful predictions of large-scale WUI fire spread by any models will be available within the next several years.

The objective of the current paper is to present a simple physics-based model that demonstrates the effect on ground-fire propagation of the winds induced by structural fires. In this proposed model, the fuel system is regarded as having two components, a surface-fuel portion consisting of grass alone and the structural fuel portion. Propagation of fires in the surface-fuel portion is treated as in the wildfire models discussed below. The structures, however, are treated as discrete fuel elements, which generate three-dimensional buoyant plumes and entrain fresh air to sustain the combustion. These entrainment winds influence the surface-fire propagation. The approximate model utilizes an empirical formula for wind-driven grass-fire spread and a physics-based analytical solution to the Euler equations to determine the ground-level wind produced by the burning structure. This simple model does not resort to a costly

Computational Fluid Dynamics (CFD) simulation. The model is based on research presented in studies reported by Rehm (2006).

In the following section of the paper, we briefly discuss physics-based models of fire behavior, focusing on those related to structure fires. Next, empirical relations and data needed for the model are given. In particular, an empirical relationship is given that relates the ROS and the local wind velocity for Australian grass fires, and also estimates are made of the heat release rate (HRR) for structural fires. Then, the coupled model is presented for the propagation of a grass fire driven by winds produced by the local meteorological conditions, entrainment flow from one or more burning houses, and from topographic features such as a hill. For the interested reader, details of the mathematical formulation of the model are given in the Appendix. Fire-front propagation for this model is illustrated by examples in the next section. Finally, discussion and conclusions are presented.

Physics-based models of fire behavior

Physics-based mathematical models of fire behavior have undergone significant development since the early 70s (Rehm 2006). These models can be divided broadly into two categories: indoor or enclosure fires, and outdoor fires. There are significant differences between these two types of fires. For example, indoor fires are generally limited by the oxygen that can reach the fire through openings in the enclosure. Outdoor fires, however, are limited by the supply of wildland fuel. Also, fuel moisture content is a critical factor controlling ignition and spread of wildfires, whereas fuel moisture content is much less important for the description of indoor fire behavior.

Here we discuss primarily models for structural fires. This limitation is introduced for two reasons. First, there are several recent papers that review models of wildfire. For example, a recent review of wildfire predictive capability by Andrews *et al*. (2007) has appeared in Scientific American. More technical reviews of wildfire models are given by Mell *et al*. (2007), Pastor *et al*. (2003) and by Perry (1998) among others.

Second, models for structural fires have been developed to deal with fires inside single or multiple enclosures, as noted above, and not to predict behavior of fully involved structural fires. We are aware of no data on burning rate or HRR for any scenario including ignition through burnout for a whole structure. Yet such information is required to develop a model for WUI fires. Acquisition of such data is very expensive as the complete burning of buildings is not generally sanctioned by fire authorities, and if sanctioned, not adequately instrumented to obtain the data required. The ignition location, the building materials, the interior fire-spread scenario, the prevailing wind conditions, and the response of the structure to severe burning conditions (such as wall, floor or ceiling penetration and collapse) would all be necessary data, for example, to adequately calibrate and test a model for a house burning down. A database to test the robustness of any outdoor structural-fire model would require many such full-scale burns. No such database exists.

Indoor fire models are further subdivided into two categories, zone models and field models. The formulation of both zone and field models start from the basic conservation laws of mass, momentum, energy and species, together with radiative transport. Zone models have been used to study fire dynamics in structures for about four decades. They take advantage of approximate mathematical submodels of the physical processes that occur in enclosure fires to simplify the conservation laws. As a result, they end up with non-linear ordinary differential equations together with complex, non-linear algebraic relations connecting dependent variables. These simplifications reduce both the data and the computational resources required to predict the progression of a fire in a structure. The model CFAST (Jones *et al*. 2004) is a recent example from National Institute of Standards and Technology (NIST) of this class of models.

Field models begin with a partial differential equations (PDEs) description of the conservation laws and radiative transport, and attempt to integrate these equations directly using techniques from CFD and other disciplines. During the past three decades, field models have been developed and applied very successfully to fires in structures. Field models require considerably more data and computational resources to make predictions and can provide substantially more detail about fire behavior than zone models. There are several examples of field models; a recent example from NIST of this class of models is the Fire Dynamics Simulator (FDS; McGrattan *et al.* 2007).

Physics-based models of wildland or outdoor fires have generally followed a similar, but somewhat delayed, evolution to that of indoor fires. The simpler models have generally been based on the Rothermel model (Rothermel 1972), which was developed over three decades ago. Field models for outdoor fires, however, have only begun serious development over the past several years (McGrattan *et al*. 1996; Linn 1997; Mell *et al*. 2007). In general, field models describing both indoor and outdoor fires have lagged in development over the simpler models owing to the previously prohibitive computer-resource requirements and the corresponding data requirements for such models.

Generally, the simple models of wildland fires treat the fuel as a locally homogeneous surface distribution of mass that varies slowly in the horizontal directions. The three-dimensional elevation of the ground surface is taken into account in determining the fire progression. However, usually, there is little consideration of the large-scale vertical distribution of the fuel, and the small-scale fuel structure is parameterized.

Heat release rates of grass and structure fires

Rehm *et al*. (2001) reviewed the literature on the potential energy content of various wildland fuels and compared these numbers with the potential energy content of structures. The purpose of that comparison was to estimate the density of structures required for the potential energy content to be equal to that of a particular wildland fuel. That work emphasized the importance of the potential energy content in the burning of structures as part of the overall energy available for combustion. However, that study did not consider any dynamical processes such as ignition of the fuels or HRRs required to sustain and propagate the fire. Furthermore, there were no estimates of the duration and completeness of the combustion processes during a WUI fire.

This section extends that previous work by considering time-dependent processes for two WUI fuels. An empirical relation for the propagation speed for grass fires is used, and the burning

times or the HRR for ventilation-controlled structure fires is estimated.

Grass fires

We utilize an empirical relationship presented in the paper of Cheney *et al*. (1998) for the ROS, r_w, of the fireline in Australian grass, in $m\,s^{-1}$. This ROS is determined as a function of the ambient wind speed, V_a, in $m\,s^{-1}$, the effective length W of the head portion of the fireline in m and the dead fuel moisture percentage M_f:

$$r_w = 0.165(1 + 3.24V_a)exp[(-0.859 - 2.04V_a)/W] \cdot exp(-0.108M_f) \quad (1)$$

For simplicity in the examples below, we have used the limit of very small moisture content and very long firelines, so that $r_w \approx 0.165(1 + 3.24V_a)$.

Structure fires

An estimate of the energy release rate during a house fire in the 1991 Oakland Hills fire was reported by Trelles and Pagni (1997). According to that estimate, a house burns at a peak rate of 45 MW for 1 h (yielding ~160 GJ), and then dies down over another 6-h period. The die-down of the fire is approximated as two steps, one 10 MW for 3 h and the last as 5 MW for 3 more hours. The total burn time is 7 h, and the total energy released by the house is 324 GJ. Assuming brush around each house, another 5 MW is released for 1 h, yielding an additional 18 GJ. (The additional HRR and total energy produced by the burning brush around the structure are included in the calculations of Trelles and Pagni (1997). However, these estimates are unnecessary for our purposes here.) If we include this additional HRR and total energy, and if the house is assumed to be 15 by 15 by 5 m, then we estimate the total potential fuel loading per unit area to be of order $1.4\,GJ\,m^{-2}$, the peak HRR per unit area to be of order $0.2\,MW\,m^{-2}$. For comparison, oil yields a heat-release rate per unit area of $\sim 2\,MW\,m^{-2}$ (see Baum *et al*. 1994; McGrattan *et al*. 1996).

Confirmation of this estimate for the magnitude of the peak HRR for a burning structure can be found in the chapter on compartment fires in the book on fire behavior by Quintiere (1997). Here, Quintiere describes the stages of a fire in a compartment and estimates the peak heating rates possible during the latter stages of a compartment fire when the fire is fully developed and the burning rate is ventilation-limited, or restricted by the amount of air entering the enclosure through the vents. During a compartment fire, the flow in and around the enclosure is driven by buoyancy, which is generated by the burning taking place both inside and outside the compartment.

In one example, Quintiere estimates a total HRR of 9 MW for a compartment in which the fuel load is taken to be proportional to the floor area, which in this case is $12\,m^2$. He points out that this peak HRR could increase to over 60 MW if the fuel was proportional not only to the floor area, but to the whole inside area of the compartment. Furthermore, a multiroom structure, with a fuel loading of the more modest type, producing 9 MW for each room, could also easily exceed the roughly 50 MW peak HRR estimated by Trelles and Pagni (1997). Therefore, based on compartment fire analysis, it seems very plausible that structure fires could have peak HRR reaching several times the estimate of 50 MW, and the duration of these peak HRR would be measured in tens of minutes to hours.

These estimates say nothing about the fact that the roof of the structure might develop a hole or even collapse under prolonged vigorous burning. In that case, the fire might then resemble more a burning crib than an enclosure fire. They also do not address the issue of the effects of winds on peak HRR or burn duration. It seems likely that winds would increase the peak HRR and reduce the burn duration, but the magnitude of these changes is not known. For our purposes here, the estimates above will be used without trying to assess these other effects.

Two comparisons can be made between structure fuels and grass fuels using the information given above and cited in the references. First, the energy density of grasses can be compared with the housing energy density. Rehm *et al*. (2002) quote Albini (1984) who gives a value of $5.5\,m\,s^{-1}$ for the ROS and a value of $1\,MW\,m^{-1}$ for the fireline intensity I of a grass fire. Using the burnable energy density of the grass as $e_g = I/\mathrm{ROS}$, we find $e_g \approx 0.2\,MJ\,m^{-2}$. For Australian grass, Mell *et al*. (2007) uses $\mathrm{ROS} = 5.5\,m\,s^{-1}$ and $I = 5\,MW\,m^{-1}$, so that $e_g \approx 1\,MJ\,m^{-2}$. These estimates can be compared with the corresponding energy density for a rectangular array of houses of specified housing density (see Rehm 2006). A housing density of 2.5 houses per hectare (1-acre lot per house), which can represent a suburban housing density in an affluent suburb, with an energy of 300 GJ per structure, yields a potential energy density $e_s \approx 75\,MJ\,m^{-2}$. A housing density of 10 houses per hectare (1/4-acre lots), which is a much more typical suburban neighborhood, yields an energy density $e_s \approx 300\,MJ\,m^{-2}$. For these housing densities, the potential energy of the structures is much higher than that of the grass.

Next, the HRR or Q_0 for grass line fires can be compared with the HRR for an array of structures (see Rehm 2006). If we take the distance between houses $\hat{L}$ as a characteristic fireline length and take 0.4-ha (1-acre) lots, then, for the structure, $Q_0 \approx 50$ MW, while for the corresponding grass-fire front, $\mathrm{HRR} \approx I \cdot \hat{L} = 64$ MW. For 0.11-ha (1/4-acre) lots, the fireline HRR is ~32 MW. The dynamics of the wind fields generated by burning fuels under low-wind conditions is determined by the HRR, and this argument demonstrates that the wildland and structure contributions to the dynamics can be comparable under common conditions.

A simple model for WUI surface-fire spread

Plume model of Baum and McCaffrey

In the paper of Baum and McCaffrey (1989), there is a fundamental analysis of the structure of a plume and its associated flow field produced by a pool fire in a quiescent atmosphere. The quiescent-atmosphere assumption implies that the plume remains upright and axially symmetric and requires that the heat release rate of the burning house produces buoyant velocities large compared with the local wind around the structure. In Baum and McCaffrey's paper, an empirical correlation for centerline temperature and velocity is determined from the compilation of data obtained from a large number of pool-fire experiments carried out by many investigators over a wide range of pool-fire

diameters. Based on the buoyant, inviscid equations of motion and this correlation, the analysis obtains the scaling relations for the characteristic length and velocity scales for a pool-fire plume. Furthermore, a detailed velocity profile is determined from a solution to these equations.

The model of Baum and McCaffrey (1989) is for a single buoyancy-driven plume in an inviscid, quiescent fluid of density ρ_0, temperature T_0 and pressure P_0 at ground level. The magnitude of the heat release rate of the source is designated as Q_0 and the specific heat of the air is denoted as C_p. The model starts with the equations for mass, momentum and energy, assuming axial symmetry. The velocity field is then decomposed into two components, one arising from the divergence and the other from the curl. The divergence of the velocity results from thermal expansion of the gas, and the curl is the vorticity, and these components can be related to the plume centerline temperature and velocity correlations. From this analysis, the following set of scaling relations arises:

$$D^* = \left(\frac{Q_0}{\rho_0 C_p T_0 \sqrt{g}}\right)^{2/5}$$
$$V^* = \sqrt{gD^*} \qquad (2)$$

where D^* = length scale (m), Q_0 = heat source (W), ρ_0 = ambient density (kg m^{-3}), C_p = specific heat at constant pressure (J kg^{-1}), T_0 = ambient temperature (in K), g = acceleration of gravity (m s^{-2}) and V^* = velocity scale (m s^{-1}).

Finally, a detailed solution for the velocity field, which is valid both inside and outside the plume, is found by Baum and McCaffrey. This velocity field at ground level is shown in Fig. 2.

Baum and McCaffrey applied their model to the study the winds generated by mass fires. The plume model was also used by Ohlemiller and Corley (1994) to estimate the thermally induced winds generated during large-scale mass-fire experiments carried out by Forestry Canada. In both cases, the estimated winds were found to be consistent with the measured winds.

Similarly, Trelles and Pagni (1997) used the model to estimate the winds generated by multiple burning houses at several times during the Oakland Hills fire of 1991. These predicted winds were then compared with measured wind data at the same times, and it was found that significant wind changes occurred, consistent with the model predictions, at nearly the same times. Specifically during the Oakland Hills fire, over a 15-min interval, from 1145 to 1200 hours on 20 October 1991, the number of houses burning was found to increase from 38 to 259, producing dramatic changes in the winds consistent with the increased burning.

The reader should note that the fire front generated by a surface fire itself also induces entrainment winds (see Dold *et al*. 2006; Mell *et al*. 2007). However, as in all of the simpler wildfire models to date, except for that of Dold, the fireline entrainment winds have not been taken into account. This approximation represents a distinct limitation of the simpler wildfire models including this proposed model. However, the proposed model represents an attempt to couple wildfire and structural fire dynamically in a model that could make predictions fast enough to be included in current operational models, such as BehavePlus (Carlton *et al*. 2004) and FARSITE (Finney 2004).

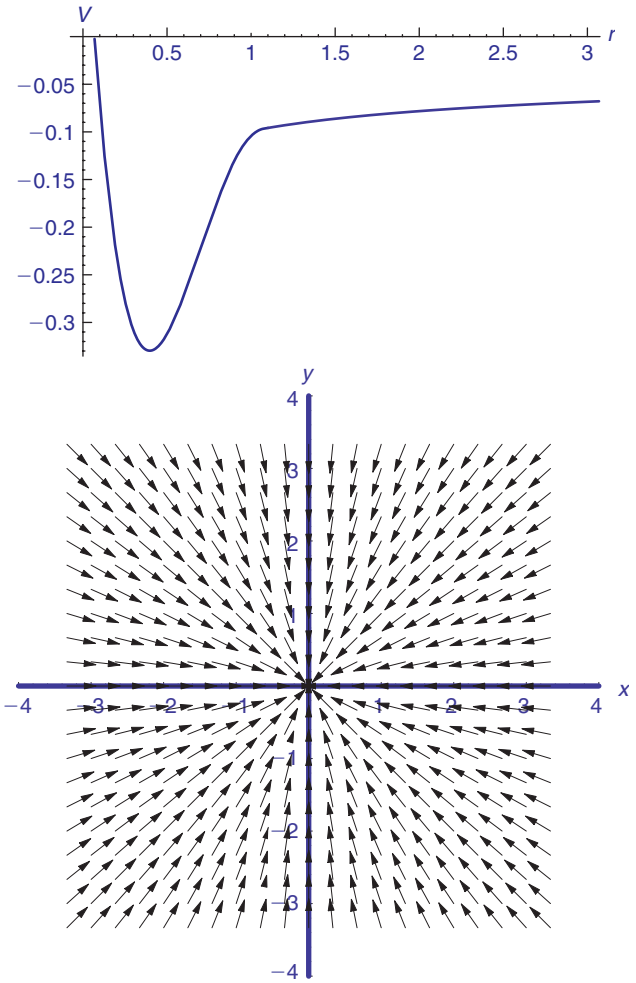

Fig. 2. Dimensionless entrainment velocity (V) at ground level induced by a structure fire (top). The velocity is plotted as a function of the radial distance (r) from the center of the structure. Dimensionless entrainment velocity vectors at ground level induced by the burning structure shown as a function of cartesian coordinates x and y (bottom). See Eqn 2 in the text for the length scale used for the non-dimensionalization.

Fire-front propagation on a three-dimensional surface

For the spread of a wildfire, it is usual to consider a fire front of arbitrary shape on a horizontal surface propagating normal to itself into unburned fuel. Behind the front, the fuel is assumed to be burned, and the front is taken to be thin relative to other dimensions of the problem. The model for the front propagation can then be formulated mathematically in two related but different descriptions. One is the so-called Lagrangian description and the other is an Eulerian description (see Sethian 1999; Fendell and Wolff 2001). In the former formulation, the advance of each Lagrangian particle on the front is related to the empirically determined normal ROS of a fire at the locally determined wind speed. This normal ROS is the local front velocity perpendicular to the front (in m s^{-1}). It is the most straightforward description and requires following only a one-dimensional, time-dependent array of these Lagrangian particles. The latter formulates the

problem as a time-dependent, convection–diffusion partial differential equation, for which the fire front at any time is a curve representing a constant value of a dependent variable of the problem. According to Sethian (1999), this formulation offers some advantages for following the front progression. However, a distinct disadvantage of this formulation is that it requires solution of a PDE in multiple spatial dimensions and time. Here we utilize the Lagrangian description.

The governing equations are the ordinary differential equations (ODEs) describing the propagation of an element of the fire front along the surface:

$$\frac{d\vec{R}}{dt} = (\vec{U} \cdot \vec{n})\vec{n} \tag{3}$$

The equations are given in vector form $\vec{R} = x(s,t)\vec{i} + y(s,t)\vec{j} + z(s,t)\vec{k}$, where $\vec{i}, \vec{j}, \vec{k}$ are unit vectors in the x, y, z directions. $\vec{U} = U_x\vec{i} + U_y\vec{j} + U_z\vec{k}$ is the ROS vector of the fire front at the location (x, y, z), and n_x, n_y, n_z are the components of the unit normal to the fire front directed toward the unburnt fuel. s is the arc length along the curve. The vector $(\vec{U} \cdot \vec{n})\vec{n}$ is the normal ROS. The model predicts the fire front propagation.

Let the height of the surface be specified as a function of the horizontal location. Then, only the first two of the three vector-component equations need to be solved because the fire-front curve is constrained to the surface. Therefore, the surface function is used to eliminate the height in the component equations for x and y, yielding two ODEs for $x(s, t)$ and $y(s, t)$. These are solved as outlined below, and the height is determined at any horizontal location from the equation for the surface.

At each point, the fire front is advanced in the direction normal to the front at a speed determined by the local ROS for the fire. This ROS depends on the local wind speed normal to the front, which depends on the ambient velocity, an equivalent topographically induced velocity and the entrainment velocities produced by all burning structures. The topographically induced wind accounts approximately for the observation that the ROS increases uphill and decreases downhill owing to buoyancy on uneven terrain (Rothermel 1972). Any local velocity induced by the fire front on itself is not taken into account. The vertical component of the velocity field is made consistent with the topography, as described in detail in the Appendix. For computational purposes, the fire front is discretized and then moved incrementally to its new location. We start with an approximation to the normal ROS, and then numerically solve the governing equations. We use the Method of Lines (MOL) and a centered difference scheme for the spatial discretization of the fire line. In the examples, we assume that the fire line initially is a straight line along the x-axis, running between $-L$ and L (see the schematic diagram in Fig. 3). Details of the mathematical equations for following the fire front are presented in the Appendix.

Model results

Fire front propagation past a burning structure

Two results using the methodology outlined above for computing a fire front propagating past a single burning structure are shown in Fig. 4. These results were reported earlier by Rehm (2006) and are given here for comparison. In the plot at the left, the fire-front progression is shown for a structure burning at 200-MW intensity with an ambient wind speed of 2 m s^{-1} blowing toward the top of the diagram. The structure is shown as a square 12 m on a side, and the fire front is shown every 25 s starting as a straight line 30 m below the center of the burning structure. The length of the initial fire line is $2L = 60$ m. For this case, the entrainment velocity produced by the burning structure accelerates the fire front as it approaches the structure and retards it after it passes. The fire front effectively spends more time in the vicinity of the burning structure.

In the plot on the right, the conditions are the same except that the fire front starts initially 10 m behind the structure; i.e. it is assumed that the peak HRR for the burning structure is achieved only after the fire front has passed it. In this case, the fire front is simply retarded by the entrainment flow as it tries to escape from the vicinity of the burning structure.

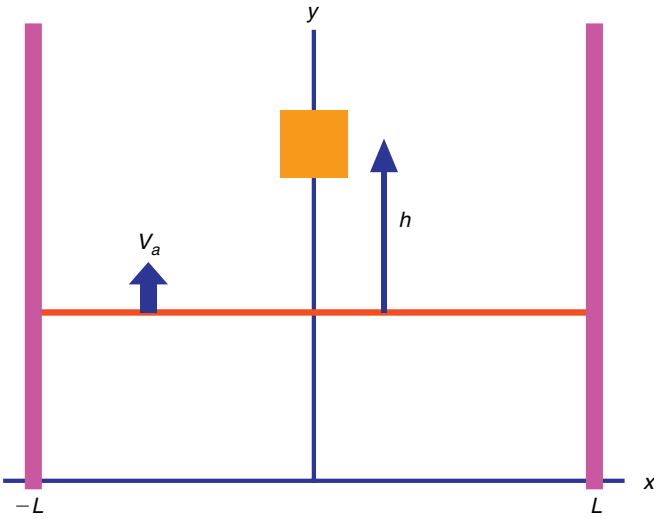

Fig. 3. A schematic diagram showing the initial location, the ambient velocity (V_a) and the extent (between the vertical bars in the x-direction) of the horizontal fire line. The burning structure is initially a vertical (y) distance h from the front.

Fire front propagation over a 2D hill with a burning structure

The next example using the methodology outlined above and presented in detail in the Appendix shows the computation of a fire front propagating along an elliptical hill in the presence of an ambient wind and the entrainment wind from a burning structure. The elevation of the hill is assumed to vary in the x- and y-directions with the functional form:

$$Z(x, y) = \frac{H}{1 + (x/W_x)^2 + (y/W_y)^2} \tag{4}$$

where H is the vertical amplitude of the hill in m, here taken to be 50 m, W_x is the length scale measured in m in the x-direction and W_y is the length scale measured in metres in the y-direction; W_x and W_y give the horizontal dimensions of the hill, each assumed to be 100 m (so the example hill is circular).

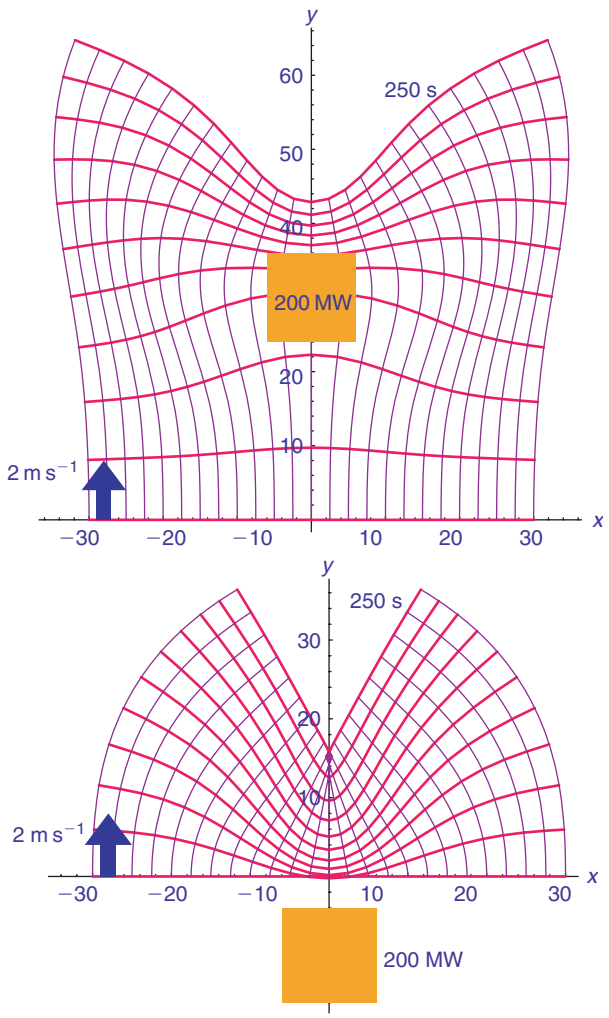

Fig. 4. The fire front at several equal time intervals for a burning structure with an ambient wind of 2 m s^{-1}, a 200 MW fire and $L = 30$ m. Distances are shown in metres. Top: House is burning before arrival of fire front. Bottom: House ignites and becomes fully involved after passage of fire front.

The equations of motion for the fire front then include an ambient wind, here assumed to be 2 m s^{-1} in the y-direction only, and an entrainment wind generated by a burning structure having an HRR of 100 MW located at $x = 0$, $y = -70$, and the effective wind generated by the topography. Fig. 5 shows the result of such a computation for which the initial fire line is located at $y = -90$ m from the peak of the hill and extends initially between $x = -30$ and $x = 30$ m in the cross-stream direction.

Fig. 5 shows the progression of the fire at equal intervals of time as it moves up the hill under the influence of three wind components, the ambient wind, the entrainment wind produced by the burning structure and the effective slope-generated wind. Using this model, the fire front progresses at a uniform speed dependent on the ambient wind in the y-direction in the absence of the hill and the burning structure. With no ambient wind and no burning structure, the model predicts that the topography-induced wind increases the ROS of the front up the hill and decreases it down the hill non-uniformly in the x-direction. Also

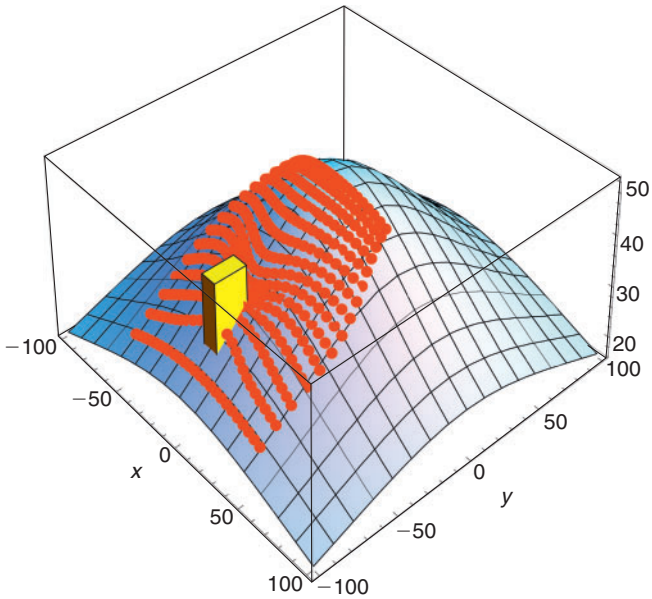

Fig. 5. The fire front at several equal time intervals propagating up a hill under an ambient wind, an entrainment wind from the burning structure and the topography-induced wind caused by the hill. Distances are measured in metres.

for this example, comparison with and without the ambient wind shows that the ambient wind increases the ROS of the front as it propagates over the hill. The entrainment wind from the burning structure accelerates the front ahead of the structure and decelerates it behind the structure non-uniformly in the x-direction.

Fire front propagation over several burning structures

Finally, we turn attention to a larger area in which there are multiple burning structures at arbitrary but specified locations. We wish to see how these burning structures can influence grass fire-front propagation as predicted by this model. We have simulated a fire front propagating on a 250 by 250 m portion of Worley, Idaho, USA, located within the Coeur d'Alene Indian Tribe Reservation Boundaries. Datasets that determine the location of non-fuel surfaces, vegetative fuels and structural fuels to 1-m or 2-m resolution for testing NIST modeling efforts have been developed under NIST sponsorship by the Coeur d'Alene Indian Tribe GIS Program. The portion of the reservation used in the present study is shown on the left of Fig. 6. The 250 by 250 m layout with eight structures is shown on the right of Fig. 6. For simplicity, we have assumed that the slightly sloped land is flat and that it is covered with Australian grass, rather than trees and roads, as shown.

The results of this simulation are shown in Fig. 7. We assumed a fireline initially 200 m long in the x-direction with an ambient wind of 2 m s^{-1} in the y-direction and that each house burned with an HRR of 100 MW. We allowed the simulation to run for 700 s of real time, requiring 423 central processing unit (CPU) seconds. The time between each fire front in the simulation plot shown in Fig. 7 was 44 s.

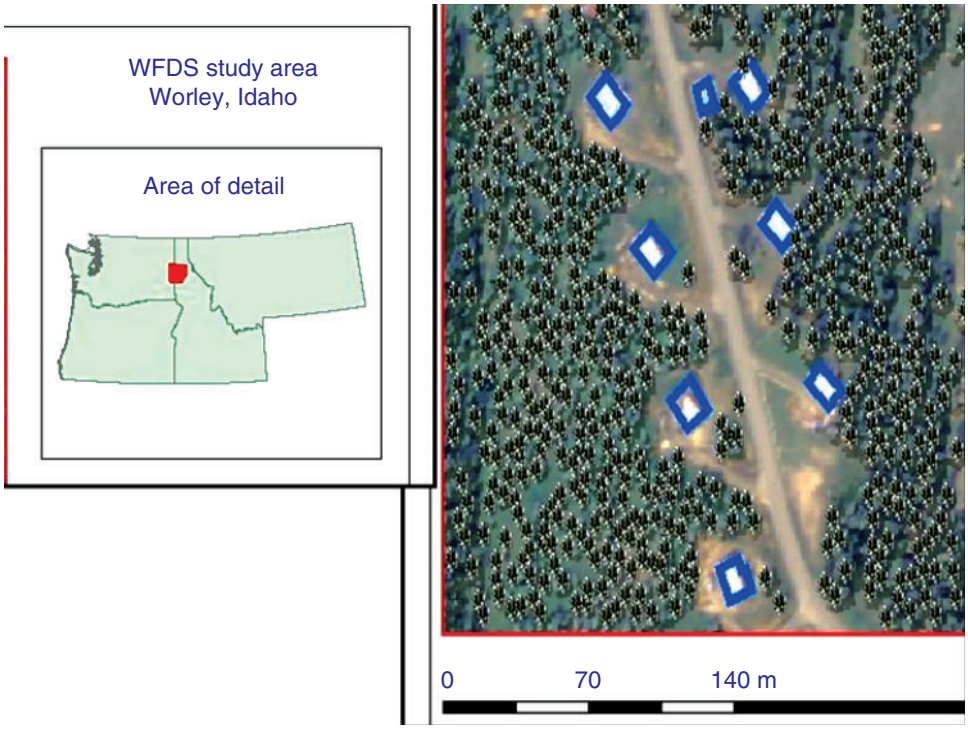

Fig. 6. Diagram showing the location of a Wildland–Urban Interface Fire Dynamics Simulator (WFDS) study area in Worley, Idaho at the left and a small section of the study area that includes the positions of eight structures. This small section is used as an example for model fire predictions in the WUI (wildland–urban interface).

In Fig. 7, note the rapid acceleration of the fire front toward the burning structures initially and the very slow progression of the front late in the simulation when the front tries to escape the influence of the eight burning structures. The net effect is for the fire front to become trapped in the vicinity of the burning structures. Therefore, it is likely that any unignited fuel in this vicinity would be exposed longer to the fire front and have an increased likelihood of ignition. The model does not address ignition or burnout of the fuels.

Discussion and conclusions

The time scale associated with burning wildland fuels is measured in tens of seconds to a few minutes. In contrast, the time scale for a burning structure is measured in tens of minutes to hours. This disparity in time scale is due, in part, to the fact that the fuel distributions for a structure and for wildland fuel differ substantially (Rehm *et al*. 2002). For a structure, for example, the fuel loading per unit area is usually much higher and its footprint much smaller than for a parcel of wildland fuel. Because of this difference, burning structures and burning wildland fuels will not couple well in general. For example, it is shown here that burning houses can substantially influence grass-fire propagation through entrainment winds. In contrast, it is not expected that burning grass, excluding its potential for ignition of the structure (which is not addressed in this model), will alter structure burning. (Fires propagating in wildland fuels will also generate entrainment winds that might influence structure fires, but this model cannot yet address this more difficult issue.)

Because of the disparity in time scales, however, it will be difficult to utilize a field model to compute multiple burning houses and vegetative (WUI) fires over large areas in any detail owing to constraints on computational resources. An advantage of this model is that it is very fast and resolves the fire front with a minimum number of nodes, even when several burning structures are assumed to be involved. All examples shown have been computed in real time or less in a computational development environment (using Mathematica; see Wolfram 1999), orders of magnitude faster than current field models. Therefore, this methodology for calculating WUI fire spread could potentially be incorporated into current operational models. Using field models for operational guidance on large-area WUI fires in the near term is unlikely.

Our analysis utilizes the plume model of Baum and McCaffrey (1989) to describe the flow field generated by a single burning house and to estimate the effects of this flow field on the progression of a surface fire. The import of the analysis, we believe, is that it demonstrates with a simple physics-based model and an inexpensive computational scheme that a house, once ignited, becomes part of the fuel system and affects fireline progression. It also allows us to investigate the changes in the fireline spread as various parameters are changed, such as the number and location of burning structures.

The HRR of a structure fire determines the strength of its plume and defines a characteristic length scale and a characteristic velocity scale for the entrainment of the plume. This model requires that the plume stand upright, and, therefore, that the ambient wind be less than the characteristic plume velocity.

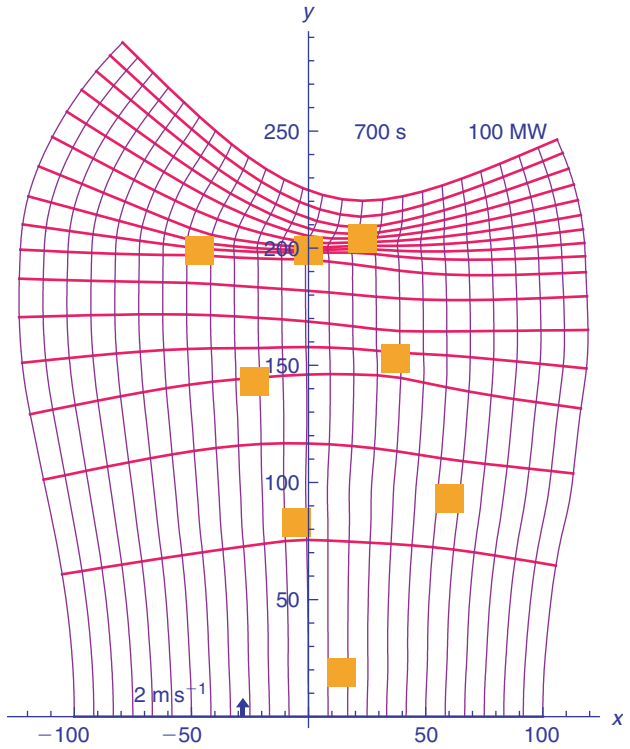

Fig. 7. The propagation of a fire front through the small area shown in Fig. 6, assuming all of the structures are burning. Distances are measured in metres.

The surface level entrainment velocity resulting from the plume model of Baum and McCaffrey (1989) decays slowly at large distances from the burning structure. The mass-fire results of Baum and McCaffrey illustrate this fact. In the present model, the slow decay can be characterized by an amplification factor, which is the ratio of the entrainment wind due to multiple burning structures to the entrainment wind produced by a single burning structure (Rehm 2006). The entrainment factor is found to grow as the HRR of each house increases, as the number of houses increases, and as the housing density increases, as discussed by Rehm (2006).

The progression of a grass-fire front (and probably other vegetation fire fronts also) can be altered substantially by burning structures as shown by the examples presented here. These examples also show that, within the limitations of this simple model, these changes can be tracked in a computationally inexpensive and robust fashion. Even though the entrainment induced by the burning grass is not taken into account in this model, several parameters determine the details of the fire-front propagation, and only a few of these variations have been examined here.

A burning structure on a hill will increase the ROS of the fire front up the hill more quickly as it approaches the structure. It will also accelerate the front non-uniformly, with greater acceleration of the front closest to the structure and less so the further the front is from the structure. Likewise, as the front recedes from the burning structure, it retards the front non-uniformly.

Finally, the entrainment caused by multiple burning structures can cause the fire front to spend significantly more time in the vicinity of these structures. The fire front is first accelerated into the vicinity of the burning structures as it approaches and then is retarded as it tries to escape the vicinity. Because of this additional time lingering near these burning structures, the fire front may tend to ignite other fuels such as nearby structures that had not been ignited previously. As noted before, however, as this simple model does not include mechanisms for ignition or burnout of the fuels, this observation is suggested, but cannot be confirmed by the model.

Acknowledgements

The present research (R.G.R.) was supported in part by NIST Contract Number SB1341–05-W-1003, Dr Anthony Hamins, Contract Monitor.

References

Albini FA (1984) Wildland fires. *American Scientist* **72**, 590–597.

Andrews P, Finney M, Fischetti M (2007) Predicting wildfires. *Scientific American* **August**, 47–55.

Baum HR, McCaffrey B (1989) Fire induced flow field – theory and experiment. In 'Fire Safety Science: Proceedings of the Second International Symposium', 13–17 June 1988, Tokyo, Japan. (Eds T Wakamatsu, Y Hasemi, A Sekizawa, PG Seeger) pp. 129–148. (International Association for Fire Safety Science and Hemisphere Publishing Corp.: New York)

Baum HR, McGrattan KB, Rehm RG (1994) Simulation of smoke plumes from large oil fires. In 'Twenty-Fifth Symposium (International) on Combustion', 31 July–5 August 1994, Irvine, CA. Vol. 25, pp. 1463–1469. (The Combustion Institute: Pittsburgh, PA)

Berry A (2007) Forest policy up in smoke: fire suppression in the United States. Property and Environmental Research Center, pp. 1–21. (Bozeman, MN) Available at http://www.perc.org/articles/article1004.php [Verified 4 May 2009]

Carlton D, Andrews P, Bevins C (2004) BehavePlus fire modeling system, user's guide, quick start tutorial. USDA Forest Service, Rocky Mountain Research Station, Systems for Environmental Management, Online Help development. Available at http://firemodels.org/content/view/12/26/ [Verified 18 May 2009]

Cheney NP, Gould JS, Catchpole WR (1998) Prediction of fire spread in grasslands. *International Journal of Wildland Fire* **8**, 1–13. doi:10.1071/WF9980001

Dold J, Zinoviev A, Weber R (2006) Non-local flow effects in bushfire spread rates. In 'V International Conference on Forest Fire Research', 27–30 November 2006, Coimbra, Portugal. (Ed. DX Viegas) (Centro de Estudos sobre Incendios Florestais: Coimbra, Portugal)

Environmental Literacy Council (2007) Forest fires. Environmental Literacy Council. (Washington, DC) Available at http://www.enviroliteracy.org/article.php/46.html [Verified 5 May 2009]

Fendell FE, Wolff MF (2001) Wind-aided fire spread. In 'Forest Fires, Behavior and Ecological Effects'. (Eds EA Johnson, K Miyanishi) Ch. 6, pp. 171–223. (Academic Press: San Diego)

Finney MA (2004) FARSITE: Fire Area Simulator – model development and evaluation. USDA Forest Service, Rocky Mountain Research Station, Research Paper RMRS-RP-4, March 1998, Revised February 2004. (Missoula, MT) Available at http://www.firemodels.org/downloads/farsite/publications/fireareaall.pdf [Verified 5 May 2009]

GAO (2005) Technology assessment; protecting structures and improving communications during wildland fires. General Accountability Office, Report GAO-05–380. (Washington, DC)

Gustafson EJ, Hammer RB, Radeloff VC, Potts RS (2005) The relationship between environmental amenities and changing human settlement patterns between 1980 and 2000 in the Midwestern USA. *Landscape Ecology* **20**, 773–789. doi:10.1007/S10980-005-2149-7

Jones WW, Peacock RD, Forney GP, Reneke PA (2004) CFAST – consolidated model of fire growth and smoke transport (version 5) technical reference guide. National Institute of Standards and Technology, Special Publication 1030. (Gaithersburg, MD) Available at http://fire.nist.gov/bfrlpubs/ [Verified 5 May 2009]

Linn RR (1997) Transport model for prediction of wildfire behavior. Los Alamos National Laboratory, Scientific Report LA13334-T. (Los Alamos, NM)

McGrattan KB, Baum HR, Rehm RG (1996) Numerical simulation of smoke plumes from large oil fires. *Atmospheric Environment* **30**, 4125–4136. doi:10.1016/1352-2310(96)00151-3

McGrattan KB, Hostikka S, Floyd JE, Baum HR, Rehm RG (2007) Fire dynamics simulator (version 5): technical reference guide. National Institute of Standards and Technology, NIST Special Publication 1018-5. (Gaithersburg, MD) Available at http://fire.nist.gov/bfrlpubs/fire07/PDF/f07048.pdf [Verified 19 May 2009]

Mell W, Jenkins MA, Gould J, Cheney P (2007) A physics-based approach to modeling grassland fires. *International Journal of Wildland Fire* **16**, 1–22. doi:10.1071/WF06002

Murphy K, Rich T, Sexton T (2007) An assessment of fuel treatment effects on fire behavior, suppression effectiveness, structure ignition on the Angora Fire. USDA Forest Service, Pacific Southwest Research Station, Report R5-TP-025. (Vallejo, CA)

National Interagency Fire Center (2006*a*) Historically Significant Wildland Fires. (Boise, ID) Available at http://www.nifc.gov/fire_info/historical_stats.htm [Verified 7 May 2009]

National Interagency Fire Center (2006*b*) Total wildland fires and acres (1960-2007). (Boise, ID) Available at http://www.nifc.gov/fire_info/fires_acres.htm [Verified 7 May 2009]

Ohlemiller T, Corley D (1994) Heat release rate and induced wind field in a large scale fire. *Combustion Science and Technology* **97**, 315–330. doi:10.1080/00102209408935383

Pastor E, Zarate L, Planas E, Arnaldos J (2003) Mathematical models and calculational systems for the study of wildland fire behaviour. *Progress in Energy and Combustion Science* **29**, 139–153. doi:10.1016/S0360-1285(03)00017-0

Perry GLW (1998) Current approaches to modelling the spread of wildland fire: a review. *Progress in Physical Geography* **22**, 222–245.

Quintiere J (1997) 'Principles of Fire Behavior.' (Delmar Publishers: Albany, NY)

Radeloff VC, Hammer RB, Stewart SI (2005) Rural and suburban sprawl in the US Midwest from 1940 to 2000 and its relation to forest fragmentation *Conservation Biology* **19**(3), 793–805. doi:10.1111/J.1523-1739.2005.00387.X

Rehm RG (2006) The effects of winds from burning structures on ground- fire propagation at the wildland–urban interface. National Institute of Standards and Technology, Report GCR 06–892, pp. 1–31. (Gaithersburg, MD)

Rehm RG, Hamins A, Baum HR, Mcgrattan KB, Evans DD (2002) Community-scale fire spread. In 'Proceedings of the California's 2001 Wildfire Conference: 10 Years after the 1991 East Bay Hills Fire', 10–12 October 2001. (Eds KS Blonski, ME Morales, TJ Morales) Oakland California Technical Report 35.01.462, pp. 126–139. (University of California Forest Products Laboratory: Richmond CA)

Rothermel RC (1972) A mathematical model for predicting fire spread in wildland fuels. USDA Forest Service, Rocky Mountain Research Station, Research Paper INT-115. (Missoula, MT)

Sethian JA (1999) 'Level Set Methods and Fast Marching Methods, Evolving Interfaces in Computational Geometry, Fluid Mechanics, Computer Vision, and Materials Science.' (Cambridge University Press: Cambridge, UK)

Trelles J, Pagni PJ (1997) Fire-induced winds in the 20 October 1991 Oakland Hills Fire. In 'Proceedings of the Fifth International Symposium for Fire Safety Sciences', 3–7 March 1997, Melbourne. (Ed. Y Hasemi) pp. 911–922. (International Association for Fire Safety Science: Boston, MA)

Wolfram S (1999) 'The Mathematica Book, 4th edn.' (Wolfram Media and Cambridge University Press: Cambridge, UK)

Manuscript received 29 May 2007, accepted 1 July 2008

Appendix

In this Appendix, Lagrangian equations are presented for determining the fire-front propagation on a specified surface or topography in the presence of burning structures. The governing equations are the ODEs describing the propagation of an element of the fire front along the surface:

$$\frac{d\vec{R}}{dt} = (\vec{U}\cdot\vec{n})\vec{n} \tag{5}$$

The equations are given in vector form $\vec{R} = x(s,t)\vec{i} + y(s,t)\vec{j} + z(s,t)\vec{k}$, where $\vec{i}, \vec{j}, \vec{k}$ are unit vectors in the x, y, z directions. $\vec{U} = U_x\vec{i} + U_y\vec{j} + U_z\vec{k}$ is the rate of spread (ROS) vector of the fire front at the location (x, y, z), and n_x, n_y, n_z are the components of the unit normal to the fire front directed toward the unburnt fuel. s is the arc length of the curve.

The linear relation given in Eqn 1 between the ROS and the local wind velocity is assumed. For a line of sufficient head width W and for very low moisture content of the grass, this reduces to:

$$U_n = ROS_0(1 + c_f V_{Tn})$$

where $U_n = \vec{U}\cdot\vec{n}$ and $V_{Tn} = \vec{V}_T\cdot\vec{n}$ with $ROS_0 = 0.165$ [m s^{-1}] and $c_f = 3.24$. Then

$$\frac{d\vec{R}}{dt} = ROS_0(1 + c_f\vec{V}_T\cdot\vec{n})\vec{n}$$

For notational simplicity, we will not explicitly show the time dependency of these functions as we obtain the tangent and the normal vectors to the fire front. The tangent to this curve is determined by $\vec{\tau} \equiv \frac{d\vec{R}}{ds}$ and can be written as:

$$\vec{\tau} = \frac{d\vec{R}}{ds} = \frac{dx}{ds}\vec{i} + \frac{dy}{ds}\vec{j} + \left(\frac{\partial Z}{\partial x}\frac{dx}{ds} + \frac{\partial Z}{\partial y}\frac{dy}{dz}\right)\vec{k} \tag{6}$$

Define the normal vector to the fire front by the parameter n as follows:

$$\vec{N} \equiv \frac{d\vec{R}}{dn} = \frac{dx}{dn}\vec{i} + \frac{dy}{dn}\vec{j} + \left(\frac{\partial Z}{\partial x}\frac{dx}{dn} + \frac{\partial Z}{\partial y}\frac{dy}{dn}\right)\vec{k} \tag{7}$$

$\vec{N}$ is determined by the requirement that the dot product of the normal and tangential vectors be zero: $\vec{\tau}\cdot\vec{N} = \frac{d\vec{R}}{ds}\cdot\frac{d\vec{R}}{dn} = 0$

Define the following quantities:

$$\frac{dZ}{ds} = \left(\frac{\partial Z}{\partial x}\frac{dx}{ds} + \frac{\partial Z}{\partial y}\frac{dy}{ds}\right) \tag{8}$$

and

$$\left(\frac{dA}{ds}\right)^2 \equiv \left(\frac{dx}{ds}\right)^2\left[1 + \left(\frac{\partial Z}{\partial y}\right)^2\right] + \left(\frac{dy}{ds}\right)^2\left[1 + \left(\frac{\partial Z}{\partial x}\right)^2\right] + \left(\frac{dZ}{ds}\right)^2\left[2 + \left(\frac{\partial Z}{\partial x}\right)^2 + \left(\frac{\partial Z}{\partial y}\right)^2\right] - 2\frac{\partial Z}{\partial x}\frac{\partial Z}{\partial y}\frac{dx}{ds}\frac{dy}{ds} \tag{9}$$

Then, we can write the unit normal vector to the fire front on the prescribed surface as follows:

$$\vec{n} \equiv \frac{\vec{N}}{|\vec{N}|} = \frac{1}{|\frac{dA}{ds}|}\left[\left(\frac{dy}{ds} + \frac{dZ}{ds}\frac{\partial Z}{\partial y}\right)\vec{i} - \left(\frac{dx}{ds} + \frac{dZ}{ds}\frac{\partial Z}{\partial x}\right)\vec{j} + \left(\frac{\partial Z}{\partial x}\frac{dy}{ds} - \frac{\partial Z}{\partial y}\frac{dx}{ds}\right)\vec{k}\right] \tag{10}$$

At the wildland–urban interface, houses as well as wildland fuels can be burning. In this model, we account for three elementary wind fields, the ambient wind, a topographically induced wind and the entrainment wind produced by all burning structures. We assume that the total velocity at any location can then be determined by adding linearly the contributions of all the elementary wind fields. The total velocity locally is taken to be the sum of these velocity contributions:

$$\begin{aligned} V_{T,x}(x,y,z) &= V_{a,x} + V_{t,x}(x,y) + V_{e,x}(x,y) \\ V_{T,y}(x,y,z) &= V_{a,y} + V_{t,y}(x,y) + V_{e,y}(x,y) \\ V_{T,z}(x,y,z) &= V_{a,z}(x,y) + V_{t,z}(x,y) + V_{e,z}(x,y) \end{aligned} \tag{11}$$

We take for simplicity the horizontal components of the local ambient wind ($V_{a,x}$, $V_{a,y}$) to be uniform in space. Then, the z-component of the ambient wind is given by $V_{a,z}(x,y) = V_{a,x}\frac{\partial Z}{\partial x} + V_{a,y}\frac{\partial Z}{\partial y}$.

In the absence of any ambient wind and over flat terrain, a fire front is found to propagate with the uniform ROS as discussed above. When there are topographical features, $Z(x,y)$, but no ambient wind, it is found that the ROS of the fire front increases uphill and decreases downhill because of buoyancy effects. This observed behavior can be treated by defining a topographically induced horizontal velocity that is proportional to the gradient of the hill (Rothermel 1972). Here, we take this equivalent horizontal velocity to be given by the relations $V_{t,x}(x,y) \equiv \alpha\frac{\partial Z}{\partial x}$ and $V_{t,y}(x,y) \equiv \alpha\frac{\partial Z}{\partial y}$, where α is a proportionality constant (Rothermel 1972). The z-component of the topographically induced velocity is given by $V_{t,z}(x,y) = V_{t,x}\frac{\partial Z}{\partial x} + V_{t,y}\frac{\partial Z}{\partial y}$.

For a fire front exposed to the velocity field generated by a single burning structure of HRR Q_0, the characteristic length and velocity scales are D^* and V^* as discussed earlier. Let $\vec{r}'$ denote the vector distance from the center of the structure to the element of the fire front. The velocity at this point will be $V_e(r') = V^*G(r'/D^*)$ where $G(r'/D^*)$ is the dimensionless velocity and D^* is the length scale defined above, and the dimensionless vector distance, $\vec{r}$, is $\vec{r} = \vec{r}'/D^*$.

The detailed solution for the dimensionless velocity function at ground level, $G(r)$ was obtained analytically by Baum and McCaffrey in terms of special functions. For computational purposes, however, this solution was replaced in the example calculations presented here by the functional form given below, which closely approximates the analytical solution:

$$G(r) = ar + br^2/2 + cr^3/3 + dr^4/4 \qquad 0 \le r \le r_0;$$

$$G(r) = ar_0 + br_0^2/2 + cr_0^3/3 + dr_0^4/4 - \frac{f_0(r-r_1)^2}{2(r_1-r_0)} + \frac{f_1(r-r_0)^2}{2(r_1-r_0)} + \frac{f_0(r_1-r_0)}{2} \qquad r_0 \le r \le r_1;$$

$$G(r) = \left[ar_0 + br_0^2/2 + cr_0^3/3 + dr_0^4/4 + \frac{(f_0+f_1)}{2(r_1-r_0)}\right]\left(\frac{r_1}{r}\right)^{(1/3)} \qquad r_1 \le r;$$

where $r_0 = 0.8$; $r_1 = 1.0$; $f_0 = 0.407199$; $f_1 = 0.045029$; $a = -2.39441$; $b = 11.2283$; $c = -13.6154$; and $d = 4.9468$.

Therefore, for a single burning structure at $(x = h, y = H)$, the induced horizontal entrainment velocity components at any point (x, y) are

$$V_{e,x} = \frac{x-h}{\sqrt{(x-h)^2+(y-H)^2}} V^* G\left(\sqrt{(x-h)^2+(y-H)^2}/D^*\right)$$
$$V_{e,y} = \frac{y-H}{\sqrt{(x-h)^2+(y-H)^2}} V^* G\left(\sqrt{(x-h)^2+(y-H)^2}/D^*\right) \quad (12)$$

The vertical component of the entrainment velocity is taken to be

$$V_{e,z}(x,y) \equiv \alpha\left(\frac{\partial Z}{\partial x} V_{e,x}(x,y) + \frac{\partial Z}{\partial v} V_{e,y}(x,y)\right)$$

The total entrainment from all of the burning structures is obtained by simple summation (Rehm 2006). If, for example, the jth structure has an entrainment velocity and a characteristic length scale determined by the heat release rate of the burning structure (as described in Rehm 2006), and if the location of the structure is given by $x = h_j$, $y = H_j$, then the total entrainment velocity is given by

$$V_{e,x}(x,y) \equiv \sum_{j=1}^{J} \frac{x-h_j}{\sqrt{(x-h_j)^2+(y-H_j)^2}} \times V_j^* G\left(\sqrt{(x-h_j)^2+(y-H_j)^2}/D_j^*\right)$$
$$V_{e,y}(x,y) \equiv \sum_{j=1}^{J} \frac{(y-H_j)}{\sqrt{(x-h_j)^2+(y-H_j)^2}} \times V_j^* G\left(\sqrt{(x-h_j)^2+(y-H_j)^2}/D_j^*\right) \quad (13)$$

where we have assumed that the entrainment velocity from each burning structure is only dependent on the vector distance in a horizontal plane between the observational location (x, y) and the location of the burning structure.

Only the first two of the three vector-component equations for the fire-front spread need to be solved, as the front is constrained to the surface $z = Z(x, y)$ (assuming that we can describe the surface explicitly in this form). The functional form for the surface is used to eliminate z in the component equations for x and y, yielding two ODEs for $x(s, t)$ and $y(s, t)$. These are solved as described below, and z is determined at (x, y) from the equation for the surface.

At each point, the fire front is advanced in the direction normal to the front at a speed determined by the local ROS for the fire. This ROS, in turn, depends on the wind speed at that location. For computational purposes, the fire front is discretized and then moved incrementally to its new location. We consider the fireline initially to be a straight line along the x-axis, running between $-L$ and L and divide this interval into $2I$ panels each of length δ, where $\delta = 1/I$. We start with an approximation to the normal ROS, and then numerically solve the governing equations. We use the MOL and a centered difference scheme for the spatial discretization at all interior nodes of the fire front. For the end nodes, we use a one-sided difference scheme with the neighboring interior node.